

A network model of parametric working memory. Supplementary Material

Paul Miller¹, Carlos D Brody², Ranulfo Romo³ and Xiao-Jing Wang¹

Part I: Spiking model network

Single neurons and synapses.

We simulate the individual cells as leaky integrate-and-fire neurons (Tuckwell 1988). The membrane potential, V_i , of cell i obeys the current balance equation:

$$C_M \frac{dV_i}{dt} = -g_L [V_i - V_L] - g_E S_{E,i} [V_i - V_E] - g_I S_{I,i} [V_i - V_I] - g_{ext} s_{ext,i} [V_i - V_E] - g_{cue} s_{cue} [V_i - V_E] \quad (1)$$

where g_L is the leak conductance, V_L the leak potential, g_E and V_E are the conductance and reversal potential for excitatory channels and g_I and V_I are the conductance and reversal potential for inhibitory channels. g_{ext} and g_{cue} are the fixed conductances for background noisy input and applied, stimulus-dependent input, respectively, while s_{ext} and s_{cue} are the corresponding time-dependent gating variables (see below). When the membrane potential reaches a threshold, V_{thr} , the neuron spikes, and the membrane potential is reset at V_{reset} for an absolute refractory period, τ_{ref} , before continuing to follow Eq.(1).

The total synaptic drive for excitation or inhibition (S_E or S_I) is the sum of synaptic inputs from all presynaptic neurons j ,

$$S_i = \sum_j W_{j \rightarrow i} s_j(t) \quad (2)$$

where $W_{j \rightarrow i}$ is the relative synaptic weight from cell j to cell i , and s_j is the synaptic current gating variable activated by the presynaptic neuron j firing spikes at times $t_{spike,j}$. Specifically, for excitatory synapses, we have

$$\frac{ds_j}{dt} = \alpha_s \cdot \overline{P_R}(t)[1 - s_j]\delta(t - t_{spike,j}) - \frac{s_j}{\tau_s} \quad (3)$$

and for inhibitory synapses:

$$\frac{ds_j}{dt} = \delta(t - t_{spike,j}) - \frac{s_j}{\tau_s} \quad (4)$$

with synaptic time constants τ_s . The probability of vesicular release, $\overline{P_R}(t)$, is described in the next subsection.

Background noisy input to all neurons is simulated using uncorrelated Poisson spike trains at a rate, r_{ext} , through non-saturating synapses, of conductance g_{ext} , which are gated according to:

$$\frac{ds_{ext}}{dt} = \delta(t - t_{spike,ext}) - \frac{s_{ext}}{\tau_{ext}} \quad (5)$$

with synaptic time constant, τ_{ext} following spikes at times, $t_{spike,ext}$.

Similarly, during the stimulus, Poisson spike trains of rate, λ , generate additional excitation through AMPAR-mediated synapses of conductance, g_{cue} , multiplied by a gating variable, s_{cue} which follows:

$$\frac{ds_{cue}}{dt} = \delta(t - t_{spike,cue}) - \frac{s_{cue}}{\tau_{ext}}. \quad (6)$$

In the network models presented here, background and stimulus inputs are mediated by AMPA receptors, with $\tau_{ext} = 2\text{ms}$, recurrent excitation through NMDA receptors with $\tau_s = 100\text{ms}$ and $V_E = 0\text{mV}$, and inhibition through GABA_A receptors with $\tau_s = 10\text{ms}$ and $V_I = -70\text{ mV}$. Other cellular parameters are for excitatory cells: $C_M = 0.5\text{nF}$, $g_L = 38.4\text{nS}$,

$V_L = -70\text{mV}$, $V_{reset} = -60\text{mV}$, $V_{thr} = -45\text{mV}$, $\tau_{ref}=2\text{ms}$, $g_{ext} = 6\text{nS}$, $r_{ext} = 1.2\text{kHz}$,
 $g_E = 36\text{nS}$, $g_I = 12\text{nS}$; and for inhibitory cells: $C_M = 0.2\text{nF}$, $g_L = 17.6\text{nS}$, $V_L = -70\text{mV}$,
 $V_{reset} = -60\text{mV}$, $V_{thr} = -50\text{mV}$, $\tau_{ref} = 1\text{ms}$, $g_{ext} = 1.6\text{nS}$, $r_{ext} = 1.8\text{kHz}$, $g_E = g_{cue} = 36\text{nS}$,
 $g_I = 12\text{nS}$.

Short-term plasticity of excitatory synapses

All excitatory synapses exhibit short-term presynaptic facilitation and depression (Varela *et al.* 1997, Hempel *et al.* 2000). We implement the scheme described by Matveev and Wang (Matveev and Wang 2000) which assumes a docked pool of vesicles containing neurotransmitter, where each released vesicle is replaced with a time constant, τ_d . The finite pool of vesicles leads to synaptic saturation, as when the presynaptic neuron fires more rapidly than vesicles are replaced, no extra excitatory transmission is possible. Such synaptic depression contributes to stabilizing persistent activity at relatively low rates.

We assume that there is at most one vesicle release per spike, hence the release probability at any individual synapse, $P_R(t)$, is

$$P_R(t) = 1 - [1 - p_v(t)]^{N(t)} \quad (7)$$

where $p_v(t)$ is the release probability for an individual vesicle and $N(t)$ is the number of docked vesicles (smaller than a maximum N_0). We make the simplification that there are many synapses between each pair of connected neurons, such that the average release probability per synapse, $\overline{P_R(t)}$, simply scales the amplitude of synaptic transmission, as shown in Eq. 3. Similarly, we do not keep track of a discrete $N(t)$ for every individual synapse, but assume that the several synapses between two neurons have a Binomial distribution with an average

number of docked vesicles, $\langle N(t) \rangle$. The brackets $\langle \rangle$ in Eq. 10 represent the average over this Binomial distribution, with mean $\langle N(t) \rangle$ and maximum N_0 . Hence $\langle N(t) \rangle$ is a continuous variable obeying:

$$\frac{d \langle N \rangle}{dt} = \frac{N_0 - \langle N \rangle}{\tau_d} - \overline{P_R(t)} \delta(t - t_{spike}) \quad (8)$$

decreasing by $\overline{P_R}$ after a spike at time t_{spike} . By averaging over the binomial distribution we have

$$\overline{P_R} = \langle 1 - [1 - p_v(t)]^{N(t)} \rangle \quad (9)$$

$$= 1 - [1 - p_v(t) \cdot \langle N(t) \rangle / N_0]^{N_0} \quad (10)$$

and this value of $\overline{P_R}$ is used in Eq. 3.

The vesicular release probability is given by the product of three gating variables, $p_v(t) = O_1(t)O_2(t)O_3(t)$. A gating variable $O_i(t)$ ($i = 1, 2, 3$) increases due to calcium influx triggered by an action potential, followed by a decay with time constant τ_f^i between spikes. Specifically, the following simple update rule is used: A gating variable $O_i(t)$ ($i = 1, 2, 3$) follows

$$O_i(n+1) = 1 - \left\{ 1 - O_i(n) \exp \left[-(t_{n+1} - t_n) / \tau_f^i \right] \right\} C_f^i \quad (11)$$

Our simulations use the following values for the parameters: $N_0 = 16$, $\tau_d = 500$ msec, $C_f^1 = 0.45$, $\tau_f^1 = 50$ msec, $C_f^2 = 0.75$, $\tau_f^2 = 200$ msec, $C_f^3 = 0.9$, $\tau_f^3 = 2$ sec.

Synaptic facilitation helps to stabilize the network to noise, because brief fluctuations in activity do not get transmitted through recurrent excitatory synapses. However, our network is not designed to use the facilitating synapses with their longer time constants as the basis of time integration (Shen 1989).

Connectivity details

Connection strengths between neurons depend only on their group numbers, and are all-to-all.

All weights are normalized (*i.e.* divided by) the number of neurons in the presynaptic group,

so that average network properties should be independent of the system size.

The set of weights W_{EI} , W_{IE} , W_{II} all follow the same form:

$$W_{i \rightarrow j}^{EI} = W_{max}^{EI} \exp\left(\frac{-|i-j|}{N_{grps}\sigma_{EI}}\right) \quad (12)$$

where $N_{grps} = 12$ is the total number of groups used, W_{max}^{EI} is the maximum connection strength, between groups of the same label ($i = j$) and σ_{EI} determines the breadth of connections to other groups. W_{max}^{IE} , σ_{IE} , W_{max}^{II} and σ_{II} have similar definitions.

The recurrent excitation has a slightly different form. First, the connections within the same group are significantly stronger than those between groups, so we define a separate set of parameters for the $W_{i \rightarrow i}^{EE} = W_i$. Second, the connection strengths between different groups i and j is asymmetric:

$$W_{i \rightarrow j}^{EE} = W_0^{EE} \exp\left(\frac{-|i-j|}{N_{grps}\sigma_i A}\right) \quad (13)$$

for $i < j$ and

$$W_{i \rightarrow j}^{EE} = W_0^{EE} \exp\left(\frac{-A|i-j|}{N_{grps}\sigma_i}\right) \quad (14)$$

if $i > j$, where $A = 1.5$ is an asymmetry factor.

The full set of parameters are as follows: $W_0^{EE} = 0.16$, $W_1 = 0.244$, $W_2 = 0.239$, $W_3 = 0.237$, $W_4 = 0.238$, $W_5 = 0.239$, $W_6 = 0.24$, $W_7 = 0.241$, $W_8 = 0.242$, $W_9 = 0.243$, $W_{10} = 0.244$, $W_{11} = 0.245$, $W_{12} = 0.246$; $\sigma_1 = 0.5$, $\sigma_2 = 0.5$, $\sigma_3 = 0.39$, $\sigma_4 = 0.385$, $\sigma_5 = 0.385$, $\sigma_6 = 0.388$, $\sigma_7 = 0.392$, $\sigma_8 = 0.397$, $\sigma_9 = 0.402$, $\sigma_{10} = 0.408$, $\sigma_{11} = 0.414$, $\sigma_{12} = 0.42$; $W_{max}^{EI} = 1.65$, $\sigma_{EI} = 0.25$, $W_{max}^{IE} = 0.5$, $\sigma_{IE} = 0.2$, $W_{max}^{II} = 2.0$, $\sigma_{II} = 0.5$.

Finally, there is cross-inhibition, such that the excitatory group i excites the oppositely monotonic inhibitory group, $14 - i$ (see Fig. 1) with strength $W_{cross}^{EI} = 0.25$.

Part II: Mean field analysis

Mean field method

We develop a mean field analysis that allows us to approximate the full spiking dynamics of a group of identical, asynchronously firing neurons by their average firing rate as a function of time. The key idea of a mean field analysis is to ignore fluctuations, and treat the system in terms of slowly-varying average quantities. In the simplest analysis which we use here, only one variable such as the firing rate is used to define the population activity. In a second order analysis (Renart *et al.* 2003b) the average fluctuations (*i.e.* variance) in the firing rate are also calculated self-consistently, such that the average CV becomes a second variable in the population dynamics. In principle higher order correlations can be included, but the calculations become overly complex to little advantage.

In other work (Brunel and Wang, 2001), analytical formulae have been developed to describe the firing rate of a leaky-integrate-and-fire neuron as a function of its excitatory and inhibitory inputs. In the present paper we develop a different, empirical approach, which is somewhat less elegant, but has computational benefits. Our reasons are two-fold. First, the analytical formula contain terms which are computationally expensive to calculate. We save time by fitting functions that are simpler. Second, the spikes of one neuron only affect another when transmitted through the recurrent synapse, where they cause a change in synaptic con-

ductance. It is the change in synaptic conductance which affects the firing of the next neuron, and must be calculated self-consistently for the network. Hence we formulate our theory in terms of the average synaptic conductances (which can be excitatory and inhibitory) rather than firing rates.

We develop our mean field analysis by simulating a single spiking neuron under various levels of constant excitation and inhibition. As well as recording the spikes for 100s, we also calculate the effect of those spikes when passed through one of the recurrent synapses of the network. Hence we know the average amount of excitatory (or inhibitory when analyzing an interneuron) conductance that such a spiking neuron contributes through recurrent connections in the network. The mean field analysis is consistent in that constant values of excitatory and inhibitory conductances (scaled as S_E, S_I) are used to excite the cell, and we use the average value of synaptic conductance from the resulting spike train (s^{out}) as the constant effect of this neuron on the rest of the network.

For each population in the network, the following steps are taken in a mean field approach (see Fig. S1):

(1) Assign total synaptic inputs.

Assign the amount of excitation ($S_{E,i}$) and inhibition ($S_{I,i}$) that each population, i , receives. These quantities scale the excitatory conductance, g_E , and inhibitory conductance, g_I , of each neuron and determine its firing rate.

(2) Generate spiking statistics (Fig. S1a).

Given the excitatory and inhibitory inputs, $S_{E,i}$ and $S_{I,i}$ to the neuron in the i -th population and including the neuron's standard Poisson noise input (see Supplementary Part I: Single neurons and synapses) we calculate the spiking statistics. We measure all spikes over

a long interval (100s) to obtain both the average rate and effectively all orders of correlations between spikes for the given inputs. Fig. S1a indicates that the principal effect of increased inhibition to a ‘standard’ leaky-integrate-and-fire neuron is a shift in the threshold of the neuron, but otherwise the firing rate curve is almost parallel.

(3) Generate average synaptic dynamics from spikes (Fig. S1b).

The spike train is passed through a standard synapse. We assume all recurrent excitatory synapses are identical in character, differing only in maximal conductance. Similarly all inhibitory synapses are identical to each other. Hence the spike train of the standard neuron in the i -th population gives rise to an average amount of gating, s_i^{out} , which describes the effect of the presynaptic neuron on all of its postsynaptic contacts.

Fig. S1b demonstrates that the firing rate of excitatory neurons, $\nu_{E,i}$, contains nearly all of the information about the effect of a neuron on the postsynaptic conductance of another ($s_{E,i}^{out}$). The reason is that when the neuron, with fixed external noise and otherwise non-fluctuating inputs, is firing at a certain rate, the CV does not greatly depend on the mixture of constant inhibition and excitation that cause that firing rate. The small difference in curves is a consequence of a slightly greater variability in spike times when firing at a particular rate in the presence of stronger synaptic inputs, which decrease the effective membrane time constant. A greater CV at a given rate leads to lower average postsynaptic conductance, s_E^{out} , for excitatory cells.

(4) Sum all synapses to obtain new total inputs.

The gating fraction, s_i^{out} must be weighted by the maximal synaptic conductance, to give its actual effect on the postsynaptic neuron. The weight depends on which populations the neurons are in, and is given by $W_{i \rightarrow j}$ for the synaptic weight of a neuron from population i

to population j . Hence we calculate the total excitation to neurons in population j as $S_{E,j} = \sum_i W_{i \rightarrow j} s_{E,i}^{out}$, where the sum over i is over all excitatory populations, and $S_{I,j} = \sum_k W_{k \rightarrow j} s_{I,k}^{out}$, where the sum over k is over all inhibitory populations.

(5) Enforce self-consistency.

The newly calculated values of excitation and inhibition for each population $\{S_{E,j}, S_{I,j}\}$ must be the same as those assigned in step (1) for a self-consistent solution. That is the values of recurrent synaptic inputs assigned in stage (1) are exactly those produced by the network as calculated in stage (5). Fig. S1c plots the same curves as Figs S1a-b, but on the axes that are used for fitting the data, as the variables S_E , S_I and s^{out} are used for each neuron in the self-consistency calculations. The average firing rates belonging to each population in the steady state are readily obtained from stage (2).

Note that our method includes the full details of the spike train, not just the average firing rate. Spike trains of the same rate but different variability result in different average conductance changes when passed through a synapse. In particular, for a saturating synapse, a regular spike train of a given rate leads to the largest average postsynaptic conductance. However, while fluctuations in spike times are included to all orders, the method is strictly first-order, as the effect of fluctuations of the synaptic conductances on the membrane potential and hence spike times is not included. Given the long synaptic time constant of 100ms for the NMDA receptors of recurrent synapses, it is certainly reasonable to expect that fluctuations in synaptic conductance are less important than fluctuations in spike times.

Fig. 6 in the main text, which shows the stable states of the network, is plotted using *Xppaut*. Two coupled networks, each of 12 excitatory populations and 12 inhibitory populations are simulated. A single mean-field neuron represents each asynchronous population

of identical neurons. The parameter that is varied in the x-axis is applied excitatory drive conductance, g_{App} . The drive is designed such that positive g_{App} makes the positively monotonic neurons more excitable, but the negatively monotonic neurons less excitable. That is $S_{E,i} \mapsto S_{E,i} + g_{App}/g_E$ for populations 1,2,...12 and $S_{E,i} \mapsto S_{E,i} - g_{App}/g_E$ for populations 1*,2*,...12*.

For our neurons, the leak potential is equal to the reversal potential of inhibitory synapses ($V_L = V_I$). Hence the firing threshold of neurons can be changed by adding a constant inhibitory conductance, $S_I \cdot g_I$, which has an effect identical to a shift in the leak conductance, g_L . So the curves of Fig. S1 are equivalent to curves of neurons with different thresholds and identical inhibitory input.

Mean field dynamics

The dynamics of $s_{E,i}^{out}$ for each mean-field excitatory neuron evolve according to the following formulae:

$$\tau_s \frac{ds_{E,i}^{out}}{dt} = -s_{E,i}^{out} + F(S_{E,i}, S_{I,i}) \quad (15)$$

where $F(S_{E,i}, S_{I,i})$, plotted in Fig. S1c and defined in the next subsection, is the stable value of $s_{E,i}^{out}$, given total excitatory inputs, $S_{E,i} = \sum_j W_{j \rightarrow i} s_{E,j}^{out}$ (where $\{j\}$ = set of E-cells) and inhibitory inputs $S_{I,i} = \sum_k W_{k \rightarrow i} s_{I,k}^{out}$ (where $\{k\}$ = set of I-cells). Similarly for inhibitory neurons,

$$\tau_s \frac{ds_{I,i}^{out}}{dt} = -s_{I,i}^{out} + G(S_{E,i}, S_{I,i}) \quad (16)$$

with $G(S_{E,i}, S_{I,i})$ defined below, and the inputs $S_{E,i}$ and $S_{I,i}$ calculated in the same way as for excitatory neurons.

The equations are simulated with the synaptic time constant, $\tau_s = 100ms$. Qualitatively all the significant behaviors of the full-spiking network, including slow time integration, can be observed in the mean field model. The .ode file used for these simulations can be downloaded from the internet at

<http://www.wanglab.brandeis.edu/~pmiller/2twlviec.ode>, and run using *Xppaut*.

Numerical approximations

In our mean field analysis, we use approximate formulae obtained by fitting suitable functions to the measured synaptic output of model neurons. More elegant, analytic expressions do exist for the firing rate and synaptic output of noisy integrate-and-fire neurons (Brunel and Wang 2001) but these expressions include complicated integrals whose calculation requires considerable time. Use of the full formulae would slow down the calculations considerably.

Fig. S1c includes the plot of the formula, $F(S_E, S_I)$ that is empirically fitted to the measured curves of excitatory synaptic output, s_E^{out} . The fitted formula is given by:

$$s_E^{out} = F(S_E, S_I) = \frac{0.742808}{4} \left\{ 1.0 + \frac{\exp[\alpha(S_E - \beta)] - 1.0}{\exp[\alpha(S_E - \beta)] + 1.0} \right\} \cdot \left\{ 1.0 + \frac{\exp[\gamma(S_E - \delta)] - 1.0}{\exp[\gamma(S_E - \delta)] + 1.0} \right\}. \quad (17)$$

The functional form was chosen to give zero in the limit of a quiescent neuron, to saturate at the correct maximum value for the depressing synapses used, and to allow different rates of curvature near minimal activity to that near saturating activity. Note that the maximum, saturating value, $s_{E,M}^{out}$ in the limit of large firing rates is given by the regular spiking result:

$$s_{E,M}^{out} = \nu_M \tau_s \frac{(1 - e^{-\alpha_s})(1 - e^{-1/\nu_M \tau_s})}{1 - e^{-\alpha_s} e^{-1/\nu_M \tau_s}} = 0.742808 \quad (18)$$

where $\nu_M = N_0/\tau_d$ is the maximal rate of vesicle release.

The coefficients $\alpha - \delta$ were calculated as a best fit for each curve with constant inhibition, then the values of these coefficients were calculated from 20 curves with different inhibitory input. Hence the coefficients themselves could be fit as functions of the inhibitory input, S_I , where the functional form was chosen by eye:

$$\alpha = 17.2065 + 13.014 \cdot \exp(-0.153926 \cdot S_I) \quad (19)$$

$$\beta = 0.0448419 + 0.158992 \cdot S_I + 0.00088194 \cdot (S_I)^2$$

$$\gamma = 12.844 - 2.10019 \cdot \exp(-0.241788 \cdot S_I)$$

$$\delta = 0.0309221 + 0.1655 \cdot S_I + 0.000711173 \cdot (S_I)^2.$$

The firing rate, ν , of excitatory neurons is not needed in the self-consistency calculation, but is used to plot the results in Fig. 6 of the main text. It is obtained from the synaptic output variable, s_E^{out} by empirically fitting a formula to Fig. S1b, giving:

$$\nu_i = 16.47 \sqrt{\frac{s_{E,i}^{out}}{0.742808 - s_{E,i}^{out}}}. \quad (20)$$

Finally, we show how we include the inhibitory effects of interneurons. The inhibitory synapses in our model do not undergo short term plasticity, so the average inhibitory postsynaptic conductance due to an interneuron is directly proportional to the average firing rate of that interneuron ($\nu_{I,i} = s_{I,i}^{out}/\tau$, where $\tau = 10\text{ms}$). The average gating is:

$$s_I^{out} = G(S_E, S_I) = 10 \cdot \left[1 - \frac{1}{1 + \epsilon(S_E - T)^4} \right] \quad (21)$$

so long as the excitatory input, S_E , is above the threshold, T , and is zero otherwise. The functions are fitted as:

$$T = -0.107738 + 0.126268 \cdot S_I + 0.000182802 \cdot (S_I)^2$$

$$\epsilon = 67.9692 - 18.8083 \cdot \exp(-0.791788 \cdot S_I).$$

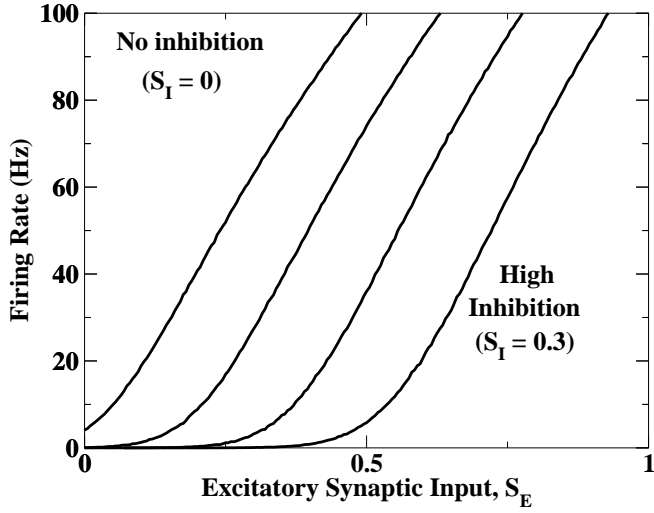
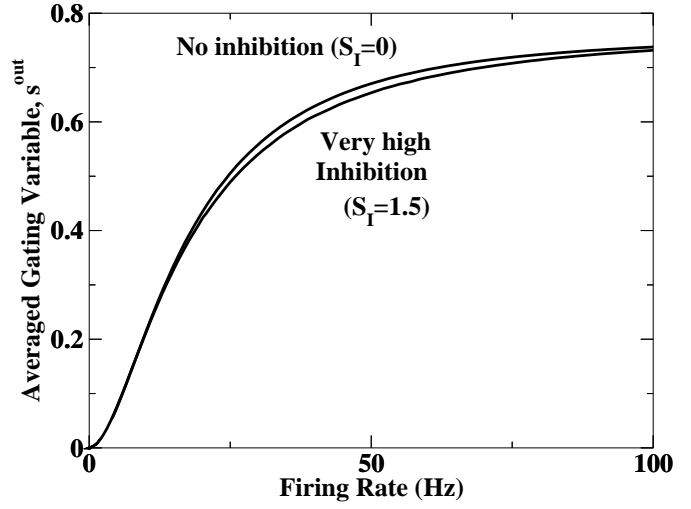
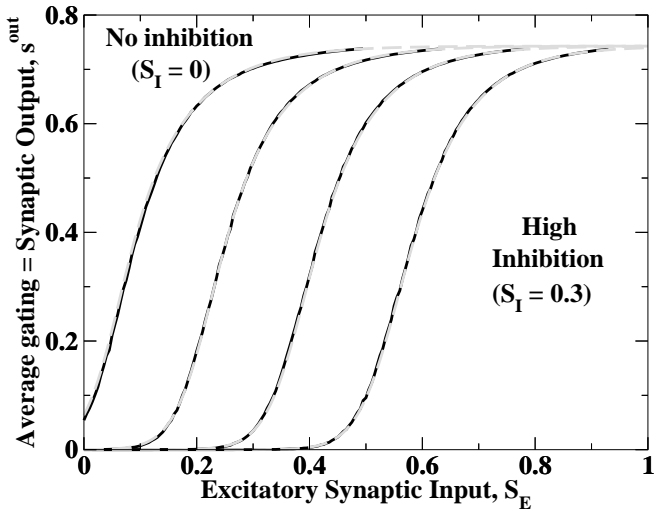
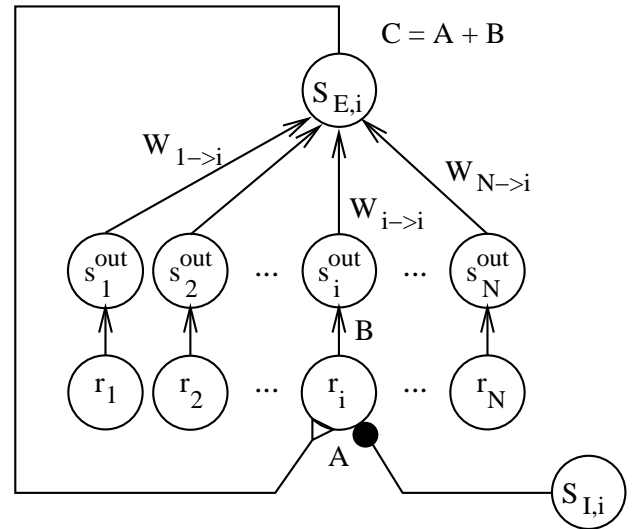
Supplementary Figure 1

(a) Firing rate of the model excitatory cell as a function of average gating, S_E through the recurrent excitatory channels of conductance, $g_E = 36\text{nS}$, with different levels of inhibitory conductance, $S_I \cdot g_I$ where $g_I = 12\text{nS}$.

(b) The spikes of the model cell lead to probabilistic release of vesicles, that gate receptors in the postsynaptic neuron. The average gating of the excitatory postsynaptic cells, s_E^{out} is plotted as a function of the firing rate of the presynaptic cell. The curves are not identical, as not only the rate, but also the correlations between spikes affect s_E^{out} .

(c) Combining curves (a) and (b) we plot the gating of the postsynaptic neuron as a function of inputs to the presynaptic neuron. These curves are fit with an empirical formula (dashed) that is used in the mean field model.

(d) Schematic figure indicating the mean field method, with stages A and B marked to indicate the corresponding figures S1(a) and S1(b). Note that $S_{E,i} = \sum_j W_{j \rightarrow i} s_{E,j}^{out}$.

A**B****C****D****Figure S1**